Chinese Chemical Letters 36 (2025) 110320

Contents lists available at ScienceDirect

Chinese Chemical Letters

journal homepage: www.elsevier.com/locate/cclet

Environmentally safe storage and sustained release of hydrogen peroxide utilizing commercial hydrogel

Zhuan Chen[a,1], Bo Yang[a,1], Jun Li[a], Kun Du[a], Jiangchen Fu[a], Xiao Wu[a], Jiazhen Cao[b], Mingyang Xing[a,b,*]

[a] Key Laboratory for Advanced Materials and Joint International Research Laboratory of Precision Chemistry and Molecular Engineering, Feringa Nobel Prize Scientist Joint Research Center, Frontiers Science Center for Materiobiology and Dynamic Chemistry, School of Chemistry & Molecular Engineering, East China University of Science and Technology, Shanghai 200237, China
[b] Shanghai Engineering Research Center for Multimedia Environmental Catalysis and Resource Utilization, East China University of Science and Technology, Shanghai 200237, China

ARTICLE INFO

Article history:
Received 28 February 2024
Revised 11 July 2024
Accepted 6 August 2024
Available online 9 August 2024

Keywords:
Hydrogel
H_2O_2 storage and transportation
Sustained release
Water remediation
Bacterial inactivation
Fenton reaction

ABSTRACT

H_2O_2 is an environmentally friendly oxidizing agent with minimal secondary pollution; however, its application has always been constrained by factors such as storage and transportation. In this study, we propose an innovative method for storing and releasing H_2O_2 using hydrogels. Commercial hydrogels (sodium polyacrylate) can undergo swelling and absorb H_2O_2 in aqueous solutions, and the swollen hydrogel can continuously release H_2O_2 under osmotic pressure. And the characteristics of osmotic pressure drive ensure the recyclability of hydrogel for H_2O_2 storage. Experimental results demonstrate that H_2O_2 can stably exist within the hydrogel for an extended period, and this strategy helps to avoid explosion the risk and potential environmental hazards during the transportation of H_2O_2. Finally, experiments confirm that the hydrogel controlled sustained release of H_2O_2 is effective in both Fenton reactions and the process of bacterial inactivation. This work introduces new ideas for the storage of H_2O_2, and the sustained release of H_2O_2 may have significant implications in the fields of healthcare, environmental science, catalysis, and beyond.

H_2O_2 is widely used as an oxidizing agent, with global demand expected to exceed 2.2 million tons per year [1]. In comparison to alternative oxidizing agents like *t*-BuOOH, N_2O, NaClO, or permanganate, H_2O_2 demonstrates a clear advantage. The reaction products of H_2O_2 mainly consist of oxygen and water, making it a more environmentally benign oxidizer compared to the mentioned agents [2–4]. The elevated reactive oxygen content of H_2O_2 (47 wt%) substantially augments its oxidizing activity. These distinctive attributes render H_2O_2 widely applicable across a spectrum of domains, including but not limited to textiles [5], papermaking [6], organic synthesis [7], biomedicine, and environmental treatment [8]. Nevertheless, H_2O_2 is a high-energy liquid fuel with exothermic reaction characteristics [9], rendering it highly susceptible to explosions and severe accidents. In recent years, there has been a notable increase in the frequency of explosion incidents involving H_2O_2 during transportation, production, and storage, posing a substantial threat to human life and property safety [10–12]. To mitigate this risk, in compliance with the International Maritime Dangerous Goods (IMDG) regulations, stabilizing agents such as phosphoric acid or phosphates are mandated to be incorporated into solutions containing H_2O_2 mass fractions exceeding 20% during transportation. Nonetheless, it is noteworthy that these stabilizers themselves present environmental concerns, contributing to eutrophication in water bodies and presenting challenges in their removal during post-treatment processes.

Hydrogel is a type of material that can absorb and swell in water. It is composed of a polymer main chain and hydrophilic functional groups, forming a three-dimensional network structure. Hydrogels have the capability to absorb water through swelling, and high-quality hydrogels can maintain favorable mechanical properties over an extended duration [13,14]. Owing to its notable attributes of high elasticity, water absorption capacity, biocompatibility, and the facile encapsulation of hydrophilic drugs, hydrogels have witnessed widespread applications across diverse domains [15–17]. Two of the most prominent roles are storage and sustained release. In agriculture, hydrogels of polyacrylamide

* Corresponding author.
E-mail address: mingyangxing@ecust.edu.cn (M. Xing).
[1] These authors contributed equally to this work.

https://doi.org/10.1016/j.cclet.2024.110320
1001-8417/

and sodium polyacrylate type are often used as water retention agents in agriculture. The hydrogel, which has dissolved and absorbed the finished water, serves as a reservoir for the soil. In instances where the soil surrounding the roots exhibits a tendency to desiccate, the water contained within the hydrogel undergoes release, facilitating plant uptake through a diffusion mechanism [16]. Furthermore, hydrogels have the capacity to absorb certain nutrients essential for plant growth [18–20]. Hydrogels which contain urea achieve the gradual release of nitrogen, thereby not only contributing to the amelioration of soil conditions but also enhancing the growth prospects of cultivated crops. Similarly, hydrogels have been applied to the storage and sustained release of other nutrients [21,22]. In the biomedical domain, hydrogels are frequently employed as carriers for pharmaceuticals and biologics as well as drug delivery [23–26]. Drug delivery systems based on hydrogels confer substantial advantages, including localized drug delivery and sustained drug release spanning days or even weeks. Due to the distinctive physicochemical properties of hydrogels, H_2O_2 may potentially be absorbed and stored within the hydrogel through its swelling capacity. However, there is currently a paucity of research in this area, necessitating a study on the mechanism of H_2O_2 storage within hydrogels.

In this study, a commercial hydrogel (superabsorbent polymer (SAP)) composed of sodium polyacrylate was employed to safely store H_2O_2. Extensive characterization *via* infrared spectroscopy, solid-state nuclear magnetic resonance (SSNMR), and X-ray photoelectron spectroscopy (XPS) confirmed sodium polyacrylate as its predominant constituent. Through testing the absorption and release of H_2O_2 by hydrogels under different conditions, the mechanism underlying H_2O_2 storage within hydrogels was elucidated and the key factors influencing the processes of H_2O_2 absorption and release was identified. Moreover, experiment was conducted to validate the stability of H_2O_2 stored within the hydrogel through stability testing. Concurrently, it was observed that SAP within the swollen H_2O_2 solution exhibited a sustained release performance, exerting a notable influence on the enhancement of pollutant degradation and the sustained bactericidal effect.

To explore the components of SAP, Fourier transform infrared (FT-IR) spectroscopy characterization was performed on sodium polyacrylate and SAP. As shown in Fig. 1a, for both sodium polyacrylate and SAP, five main peaks were observed around 3480, 2950, 1710, 1450, and 1150 cm^{-1}. The broad and intense stretching vibration band centered at 3480 cm^{-1} was attributed to the -OH group in the -COOH [27]. The peak at 2950 cm^{-1} was due to the stretching vibration of methylene (-CH_2-) in the alkyl chain. The band at 1710 cm^{-1} was assigned to the C=O stretching vibration of the -COOH group [28], the band around 1450 cm^{-1} corresponded to the asymmetric stretching vibration of the C=O group in -CO-O- [29], and the peak near 1175 cm^{-1} corresponds to the stretching vibration of -CO-O- in acrylic acid [28,30]. Through the comparison of the FT-IR spectroscopy of SAP and sodium polyacrylate, the peak positions were identical, confirming that the main component of commercial SAP was sodium polyacrylate.

To further verify the main components in SAP, SSNMR characterization of sodium polyacrylate and SAP was conducted, as shown in Fig. 1b, with peak positions roughly the same. Both sodium polyacrylate standard samples and SAP exhibited six sets of peaks, corresponding to the three standard peaks of the sodium polyacrylate sample, as well as the three standard peaks of the unpolymerized sodium acrylate monomers in the precursor [31,32]. Furthermore, in the FT-IR spectroscopy, the peaks around 1175 cm^{-1} observed in both sodium polyacrylate and SAP spectra were attributed to the stretching vibration of -CO-O- in acrylic acid, aligning with the findings from SSNMR. XPS characterization of both samples (Figs. 1c and d) also yielded the same conclusion: The main component of SAP was sodium polyacrylate.

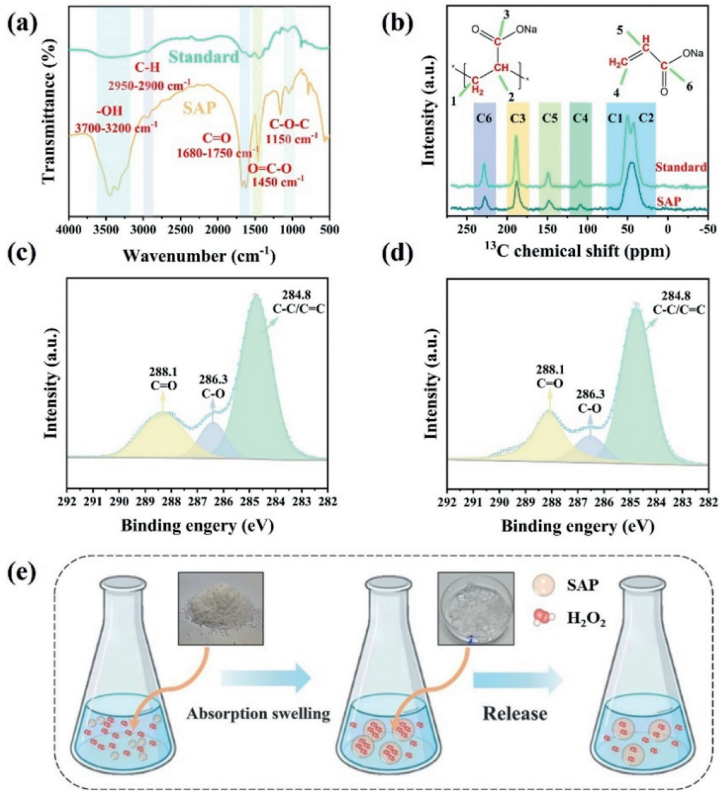

Fig. 1. (a) FTIR spectra of standard sodium polyacrylate and commercialized SAP. (b) ^{13}C NMR spectra of standard PAA and commercialized SAP. (c) SAP and (d) PAA XPS characterization. (e) Schematic diagram of SAP swell and release of H_2O_2.

As shown in Fig. S1 (Supporting information), the surface of the un-swelling SAP exhibited a rough texture, and numerous pores were present on the SAP surface, with pore sizes generally distributed between 25 μm and 70 μm. This porous structure facilitated the rapid expansion and absorption of SAP, thereby enhancing its swelling coefficient [33].

In order to evaluate the swelling and absorption properties of SAP in relation to hydrogen peroxide, along with its subsequent release capability, an experimental investigation was conducted in accordance with the outlined procedure depicted in Fig. 1e and Fig. S2 (Supporting information). As depicted in Fig. S3 (Supporting information), the solid mass (m_s) of the swollen SAP escalates with prolonged swelling duration. Notably, after 60 min, the increase in m_s becomes marginal, and by 120 min, it remains unchanged. Consequently, a duration of 2 h was deemed optimal for the swelling experiment. As described in the supporting information, the mass of H_2O_2 in SAP and the mass of H_2O_2 in the solution were determined by colorimetry, and detailed related steps were listed in Supporting information and Fig. S4 (Supporting information). The strength of SAP's ability to swell and absorb hydrogen peroxide was characterized by the dissolution coefficients swelling ratio (SR, by Eq. S1 in Supporting information) and absorption factor (Eq. S2 in Supporting information). The SR is defined as the mass of solution that can be absorbed per unit mass of SAP. The AF is defined as the mass of H_2O_2 that can be absorbed per unit mass of SAP.

The cumulative release fraction of H_2O_2 was used to investigate the H_2O_2 release process in SAP. Where the final cumulative release fraction (f_e) denotes the ratio of the mass of H_2O_2 released from SAP to the total mass of hydrogen peroxide in SAP after the equilibrium release of SAP, and is calculated as Eq. S3 (Supporting information); the cumulative release fraction at time t (f_t) denotes the ratio of the mass of H_2O_2 released from SAP to the total mass of hydrogen peroxide in SAP at time t, and is calculated as Eq. S4 (Supporting information). Similarly, when investigating release kinetics, the experiment assessed release duration *via* the variation in the cumulative release rate, denoted as f_t. As depicted in Fig. S5 (Supporting information), during the release process in ultra-pure water, f_t exhibits a continuous increase over time, plateauing around 120 min with negligible further alteration. Consequently, 2 h was designated as the duration for the release experiment.

In the experiment, SAP was placed in H_2O_2 solutions of different mass fraction to observe its swelling process and record its absorption of H_2O_2. As illustrated in Fig. S6 (Supporting information), after complete swelling in H_2O_2 solution, the mass and volume of SAP significantly increased. The experimental results, as shown in Fig. 2a, indicated that as the concentration of H_2O_2 solution increased, the SR of SAP decreased from 299.76 g/g_{sap} to 203.20 g/g_{sap}. As illustrated in Fig. 2b, with the elevation in H_2O_2 concentration, the mass of H_2O_2 absorbed per unit mass of SAP increased. The corresponding AF, calculated as per Eq. S2, for the mass of H_2O_2 absorbed per gram of SAP, correspondingly rose from 14.68 g/g_{sap} to 63.16 g/g_{sap}.

To investigate the transport, storage, absorption, and release performance of H_2O_2 with SAP as supporter under different temperature conditions, SAP was placed in various temperature environments and observed its absorption and release behavior with H_2O_2 solution. As shown in Fig. 2c, when the ambient temperatures were 4, 20, 30, and 40 °C, the AF of SAP for 20% H_2O_2 solution (20-SAP) remained nearly unchanged. Simultaneously, under different temperature conditions, 50 mg of SAP was swollen and absorbed in a 20% H_2O_2 solution and the swollen SAP was placed in 30 mL of deionized water at 20 °C. When H_2O_2 reached a balance between absorption and release, the final cumulative release fraction of H_2O_2 (f_e, by Eq. S3) in Fig. 2d showed no significant variation. Therefore, swelling H_2O_2 at different temperatures did not affect the release process of H_2O_2 from SAP. Similarly, the experiment also investigated whether temperature changes during the release process would affect the release of H_2O_2 in SAP. As shown in Fig. 2e, the f_e of 20-SAP showed no significant change under different temperature conditions. Through differential thermal analysis (DTA) experiments on 20-SAP and SAP swelling with H_2O, as shown in Fig. S7 (Supporting information), it could be observed that compared to SAP swelling with H_2O, 20-SAP has a higher temperature for the thermal absorption peak and exhibited two distinct thermal absorption peaks. This indicated that SAP has a certain temperature-stabilizing effect on H_2O_2 [34]. Based on the

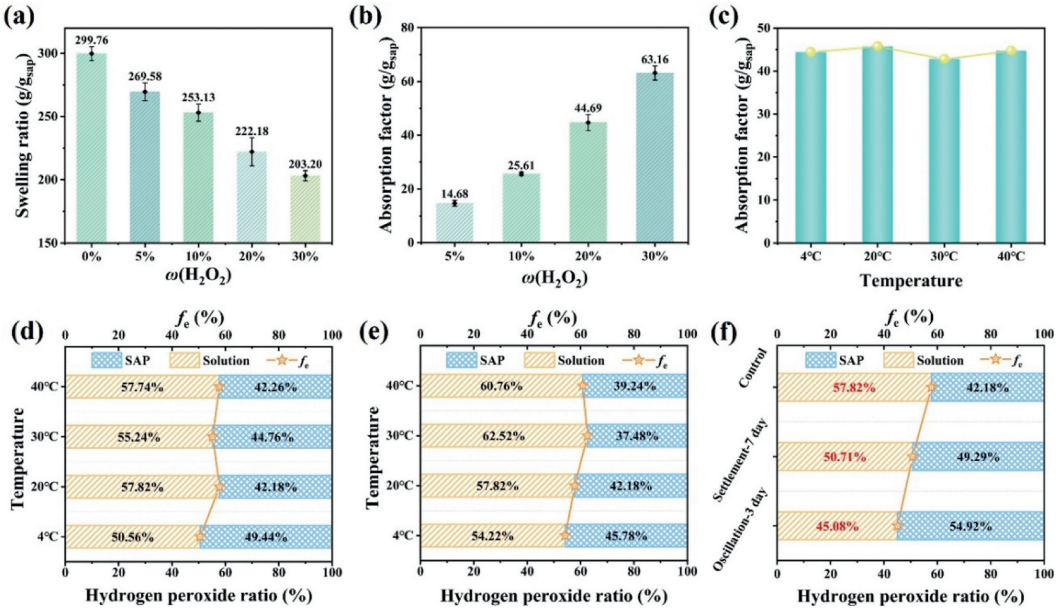

Fig. 2. (a) SR of SAP in different mass fraction of H_2O_2 solutions. (b) AF of SAP in different mass fraction of H_2O_2 solutions. (c) AF of SAP swollen 20% H_2O_2 at different temperatures. (d) The percentage of H_2O_2 released at 20 °C, by 20-SAP obtained by swelling and absorption at different temperatures. (e) The percentage of H_2O_2 released at different temperatures by 20-SAP obtained by swelling and absorption at 20 °C. (f) The percentage of H_2O_2 released after different treatment methods.

experiment above, SAP could absorb and release H_2O_2 solutions under different temperature conditions with good versatility.

In the actual transportation process of H_2O_2 solution, the potential risk of explosion existed due to factors such as friction and collision, leading to the accelerated decomposition of H_2O_2. To simulate the transportation process, 20-SAP was placed on a shaker. Under constant temperature conditions at 30 °C with oscillation speed of 160 rpm/min, the morphological changes of SAP and the release of H_2O_2 after treatment was observed. As depicted in Fig. S8 (Supporting information), when subjected to static conditions, the structural integrity of the swollen SAP remained intact for a duration of 7 days, following which notable liquefaction occurred. The mechanical structure of SAP could be maintained for >3 days under continuous vigorous oscillation conditions. As shown in Fig. 2f, the f_e of 20-SAP after oscillatory and static treatments was slightly reduced compared to normal conditions. As shown in Fig. S9 (Supporting information), the 20-SAP subjected to oscillation for 3 days still exhibited the capability to the degradation of rhodamine B (RhB) through the Fenton reaction, and its degradation performance showed no significant difference compared to the statically treated 20-SAP. The degradation effect was comparable to that of untreated 20-SAP. In the oscillation process, H_2O_2 could undergo spontaneous decomposition, resulting in a slight decrease in the f_e of SAP. And during the decomposition process, radicals from H_2O_2 could be generated, damaging the chemical bonds of SAP and causing structural breakdown. Therefore, oscillation does indeed have a certain degree of impact on the stability of SAP. However, based on the experimental results mentioned above, storing H_2O_2 with SAP can meet the transportation requirements for a certain distance. In addition, given modern transportation, 3 days is enough to safely transport H_2O_2 around the world.

H_2O_2, as a highly hydrophilic substance, served both as a donor and acceptor of hydrogen bonds. Hydrogen bonding, being an indispensable force of interaction, could potentially be one of the factors influencing both the absorption of H_2O_2 by SAP and the structural stability of SAP itself. To test this hypothesis, NaF was employed to disrupt the hydrogen bonding between SAP and H_2O_2 including NaCl in the control group for comparison. F^- could break the hydrogen bonds between O atom and H atom, forming hydrogen bonds between F and H [35]. If hydrogen bonding is the main factor facilitating SAP in absorbing H_2O_2, the binding affinity between SAP and H_2O_2 would probably decrease significantly with the addition of F^-. As a result, more H_2O_2 is likely to be released from the SAP. 5-SAP, 10-SAP, 20-SAP, and 30-SAP were placed in 30 mL of deionized water containing 1×10^{-4} mol NaF or NaCl. According to the results in Fig. 3a, there was no significant difference in the f_e of different SAP. This indicated that NaF did not result in a greater release of H_2O_2 and hydrogen bonding could not be the key factor for SAP to absorb H_2O_2. On the other hand, the f_e of each SAP sample showed an increasing trend after the addition of inorganic salts during the H_2O_2 release process.

To further investigate the impact of inorganic salts on SAP-mediated H_2O_2 release, Na_2SO_4 and KF were dissolved as solutes in the water environment where SAP released H_2O_2. For differ-

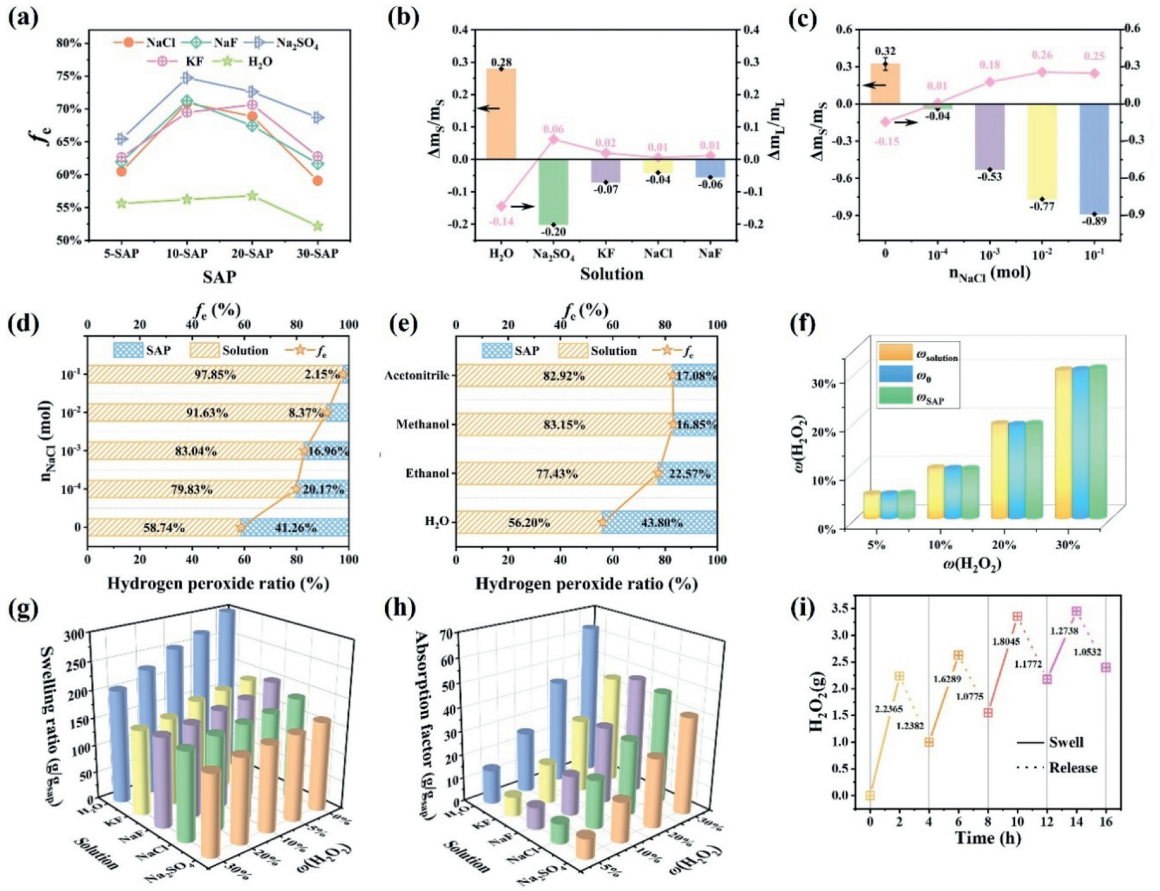

Fig. 3. (a) The final cumulative release fraction (f_e) of 5-SAP, 10-SAP, 20-SAP, and 30-SAP in different inorganic salt solutions. (b) The change of solid and liquid mass when 20-SAP is released in different inorganic salt solutions. (c) The change of solid and liquid mass when 20-SAP is released in different concentrations of NaCl solutions. (d) The percentage of H_2O_2 released in different concentrations of NaCl solutions by 20-SAP. (e) The percentage of H_2O_2 released in 30 mL of different solvents by 20-SAP. (f) Changes in ω_0, ω_{SAP}, and $\omega_{solution}$, in the process of swelling of SAP in varying mass fraction of H_2O_2. (g) SR of SAP in different H_2O_2 salt solutions. (h) AF of SAP in different H_2O_2 salt solutions. (i) SAP absorption swelling 20% hydrogen peroxide cycle test.

ent SAP samples, the f_e was highest when Na_2SO_4 was used as the solute. Simultaneously, there was no significant difference in f_e between the KF experimental group and the NaCl experimental group, ruling out the influence of cations. In the Na_2SO_4 solution, the number of solute particles per unit volume was 1.5 times that of KF/NaCl/NaF solution according to the stoichiometric ratio of substances. The number of particles in the solution greatly affects the osmotic pressure of the solution relative to the hydrogel. According to van't Hoff's osmotic pressure law, the osmotic pressure of a solution was directly proportional to the number of solute particles. As seen in Fig. 3b, the mass of 20-SAP decreased after the addition of inorganic salts and same phenomenon existed in SAP that swells with other mass fraction of H_2O_2 solution (Fig. S10 in Supporting information). Combining the results from Figs. 3a and b, when there were more particles in the environmental solution, water in the SAP was more likely to be released. At the same time, the higher the mass of water lost from the SAP, the higher f_e of SAP. Therefore, the conclusion could be drawn that the osmotic pressure of the environmental solution was an important influencing factor in the process of SAP releasing H_2O_2. Therefore, osmotic pressure was likely a key factor influencing the SAP-mediated H_2O_2 release process. To further verify that osmotic pressure was a crucial factor influencing the process of SAP absorption and release of H_2O_2, experiments were conducted to measure the f_e of H_2O_2 by 20-SAP in NaCl solutions of different concentrations. As shown in Figs. 3c and d, with an increase in the concentration of added NaCl, the mass loss of 20-SAP mass became more pronounced, and the f_e of H_2O_2 from 20-SAP also raised accordingly.

Depending on the results above, 20-SAP was further placed in 30 mL of different polar solvents, including acetonitrile, ethanol, and methanol. As shown in Fig. 3e, in these experiments, the f_e of H_2O_2 from 20-SAP was significantly higher than its release in deionized water. Meanwhile, the solid mass of 20-SAP after release in acetonitrile, ethanol, and methanol was only about 3% of the initial mass. This further indicated that the difference in osmotic pressure was the primary driving force for the release of H_2O_2, rather than hydrogen bonding. While these three solvents possess the capacity to establish hydrogen bonds with both water and H_2O_2, experimental results (Fig. S11 in Supporting information) indicate that SAP does not exhibit swelling behavior in these solvents. Therefore, during the process of H_2O_2 release, acetonitrile, ethanol, and methanol are unable to penetrate the interior of SAP, leading to a continuous osmotic pressure difference between the inside and outside of SAP. Therefore, SAP needed to continuously release ions and H_2O_2 to achieve osmotic balance inside and outside. This resulted in the substantial release of H_2O_2 and H_2O from SAP.

According to the Flory-Huggins thermodynamic theory [36], the water absorption performance of SAP depended on three key factors: (1) The number of charges fixed on SAP when it was not swollen and the osmotic pressure difference with the external solution; (2) the affinity between SAP and the solution; (3) the crosslinking density of SAP. The first part of this theory closely aligns with the observed results in the experimental findings depicted in Figs. 3a and b. The number of the fixed charges in SAP will affect the degree of SAP swelling. Simultaneously, the quantity of particles inherent in SAP and the particle count in the surrounding solution will significantly impact the osmotic pressure factor. The second part of this theory was consistent with the experimental results in Fig. S11; SAP has low affinity for acetonitrile, ethanol, and methanol. Therefore, swelling does not occur. At the same time, due to the osmotic pressure difference that always existed in the system and the hydrogen bonding between these three solutions and H_2O, H_2O and H_2O_2 in SAP were continually released.

The experiment also investigated the influence of salts on the absorption process. During the swelling and absorption process of SAP in different mass fraction of H_2O_2 solutions, the mass fraction of H_2O_2 in the original solution (ω_0), the mass fraction of H_2O_2 in SAP after swelling absorption (ω_{SAP}), and the mass fraction of H_2O_2 in the remaining liquid ($\omega_{solution}$) were calculated. As shown in Fig. 3f, the trends of these three parameters were generally consistent. When the solute particles in the exogenous solution consist solely of H_2O_2, the osmotic pressure is related only to the concentration of H_2O_2 particles in the solution. Therefore, at the end of the swelling absorption process, when osmotic pressure equilibrium is reached, the concentration of H_2O_2 inside and outside the SAP is the same and corresponds to the mass fraction of the initially added hydrogen peroxide solution.

In 30 mL of H_2O_2 solutions with different H_2O_2 mass fractions, 1×10^{-4} mol of NaCl, NaF, Na_2SO_4, and KF were added. SAP was then introduced into these solutions, and swelling absorption was carried out for 2 h. As shown in Fig. 3g, the SR decreased with the increase in the external osmotic pressure. In deionized water, the SR is the highest, reaching up to 299.76 g/g_{sap}. Conversely, the lowest SR was observed in the 30% H_2O_2 solution with the addition of Na_2SO_4, decreasing by 52.26% compared to SR in deionized water. The trend of the AF also exhibited a similar change, with SAP showing a significant reduction in AF for solutions of various H_2O_2 mass fraction upon the addition of inorganic salts (Fig. 3h). Taking a 30% hydrogen peroxide solution as an example, the mass of hydrogen peroxide absorbed per unit mass of SAP decreased by 35.68% after the addition of Na_2SO_4. After swelling in solutions with different ions, the SAP was characterized by infrared spectroscopy. As shown in Fig. S12 (Supporting information), there were no significant differences in the characteristic peaks of functional groups such as C=O and -OH. This indicates that the introduction of ions does not affect the functional groups of SAP, nor does it affect the swelling ratio of SAP through changes in ion functional groups. This further confirmed that osmotic pressure was the main driving mechanism for SAP absorption and release of H_2O_2.

The quantity of H_2O_2 within the hydrogel can be regulated by osmotic pressure, implying that the stored H_2O_2 can continuously be released and absorbed. Therefore, the subsequent experiments validated the recyclability of the SAP in absorbing and releasing H_2O_2. As shown in Fig. 3i, during four cycles of absorbing and releasing H_2O_2, SAP exhibited excellent stability. In these four cycles of experiments, the mass of released H_2O_2 by SAP showed only minor differences each time. On the other hand, the mass of SAP underwent regular changes with the absorption and release of H_2O_2. Scanning electron microscope (SEM) and FT-IR characterization of the post-cycle SAP revealed that changes in SAP before and after the cycle experiment were negligible. As shown in Figs. S13a and b (Supporting information), the size of SAP remained around 50 μm, consistent with pre-experiment measurements (Fig. S1). The FT-IR characterization of SAP before and after the cyclic experiment is presented in Fig. S13c (Supporting information), where the tensile vibration peak of SAP methylene (-CH_2-) was enhanced post-cycle. This enhancement is likely due to hydrogen peroxide reacting with residual double bonds in SAP, causing chain scission, creating and exposing additional -CH_2- groups, thereby intensifying the peak. And the mass variations of SAP in each cycle of the experiment were similar (Fig. S14 in Supporting information), providing indirect evidence of the stability of SAP during the cyclic experiments.

The relationship between the cumulative release fraction of H_2O_2 (f_t, by Eq. S4) in swollen SAP and time was also investigated. Theoretically, osmotic pressure could lead to the sustained release of H_2O_2 in SAP. To analyze the mechanism of H_2O_2 release in SAP, this study drew inspiration from three commonly used models in pharmacokinetic research: The first-order kinetic model, the Hixson-Crowell cube root model, and the Higuchi kinetic model [37]. As illustrated in Fig. 4a, the Hixson-Crowell cube root equa-

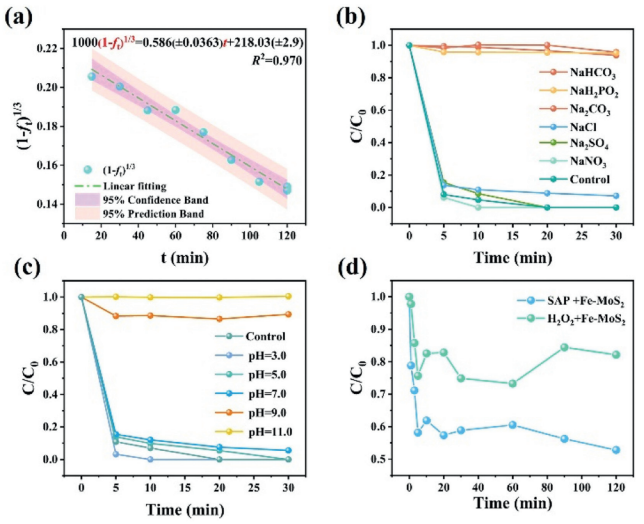

Fig. 4. (a) Hixson-Crowell cube root model kinetic release of H_2O_2. (b) The mass of H_2O_2 stored in the 50 mg hydrogel during the cycle experiment ($\omega(H_2O_2) = 20\%$). (c) Removal efficiencies of RhB (8 mg 20-SAP + 5 mg $FeSO_4{\cdot}7H_2O$) in different pH solutions ([RhB] = 20 mg/L). (d) Removal efficiencies of RhB (8 mg 20-SAP + 5 mg $FeSO_4{\cdot}7H_2O$) in different inorganic salt solutions ([Inorganic salt] = 10 mmol/L, [RhB] = 20 mg/L); and removal efficiencies of sulfadiazine (9.9 mg 30-SAP + 10 mg Fe-MoS_2 and 9 μL 30-SAP + 10 mg Fe-MoS_2) in a 10 mg/L sulfadiazine solution.

tion demonstrated the best dynamic fitting performance during the sustained release phase, with an R^2 value reaching 0.970. The Hixson-Crowell cube root equation indicated that during the release process, the diameter or volume of solid particles changed over time, consistent with the observed increase in volume during SAP release. In contrast, the R^2 values for the first-order kinetic model and the Higuchi kinetic model were relatively lower (Fig. S15 in Supporting information), indicating poorer fitting performance. Overall, the Hixson-Crowell cube root model aligned better with the process of SAP releasing H_2O_2. And The release characteristics are related to the initial mass fraction of hydrogen peroxide, specifically referring to the concentration difference of hydrogen peroxide inside and outside the SAP [37,38]. As the concentration difference increases, the release rate also increases. As shown in Fig. S5, during the release process of 30-SAP, the initial release rate is very fast. However, as the concentration difference between the inside and outside of the SAP decreases, its release rate also decreases.

The above experimental results indicated that SAP could effectively store H_2O_2, and the stored H_2O_2 could gradually release under conditions of low external osmotic pressure. Leveraging this characteristic of SAP, H_2O_2 swelling SAP could be utilized in advanced oxidation processes and bacterial deactivation procedures.

The experiment initially validated the actual release of H_2O_2 from SAP and its reaction with substances in the environmental solution through the degradation of the model pollutant RhB. This had significant implications for the widespread application of the Fenton reaction in the degradation of organic compounds. In the experiment, 20-SAP (containing 7.5 μL of H_2O_2 solution from 20% H_2O_2) and 5 mg $FeSO_4{\cdot}7H_2O$ were added to a 100 mL solution of 20 mg/L RhB. As shown in Fig. 4b, the degradation rate of RhB reached 100% within 30 min under conditions. And when NaCl, Na_2SO4, and $NaNO_3$ were added to RhB solution, it was found that the degradation effect was not significantly different compared with that without inorganic salts. This is because both the 8 mg of 20-SAP and the amount of hydrogen peroxide used are in very small quantities relative to the 100 mL of organic pollutant solution being degraded. The release equilibrium is rapidly achieved regardless of the presence of inorganic salts, and hydrogen peroxide continues to be released from the SAP only as it is consumed during the reaction.

However, degradation rate of RhB decreased under alkaline conditions, attributed to the precipitation formed by the reaction between Fe^{2+} and OH^- under alkaline conditions, hindering the effective activation of H_2O_2 for the degradation of organic pollutants. Upon the addition of various salts in Fig. 4c, it was observed that NaCl, Na_2SO_4, and $NaNO_3$ had minimal impact on the degradation process. The addition of $NaHCO_3$, NaH_2PO_2, and Na_2CO_3 significantly impacted the degradation of RhB. This was be attributed to the introduction of inorganic salts causing a variation in the pH of the reaction system. Furthermore, the incorporation of different anions could lead to the transformation of free radicals in the degradation system into radicals with lower oxidative capabilities. Simultaneously, anions also deactivated due to their reaction with Fe^{2+} [39]. As illustrated in Fig. S16 (Supporting information), this is consistent with the homogeneous Fenton reaction.

Additionally, experiments combined 20-SAP with Fe^{2+} to degrade organic pollutants such as AO7, malachite green, methylene blue, crystal violet, and phenol using the Fenton reaction. As shown in Fig. S17 (Supporting information), there was no significant difference in the degradation of various organic pollutants between the addition of 20-SAP and the direct addition of hydrogen peroxide solution. This suggests the potential application of H_2O_2 stored by SAP in Fenton reactions.

Previous research has shown that adopting a strategy of "small amount for multiple times" H_2O_2 feeding way not only developed the degradation rate of model pollutants but also significantly improved the utilization of H_2O_2 [40]. The SAP swelling with H_2O_2 solution demonstrated a characteristic of controlled H_2O_2 release in deionized water. This sustained release was beneficial for gradually providing oxidants in Fenton and Fenton-like reactions. As shown in Fig. 4d, the degradation rate of sulfadiazine was significantly increased by the SAP+Fe-MoS_2 system compared with the one-time addition of H_2O_2 (H_2O_2+Fe-MoS_2), and the degradation rate reached 2.6 times.

The controlled release function of SAP for H_2O_2 demonstrated an ideal effect in the process of long-term sterilization and disinfection. In this study, the paper disc diffusion method was employed as the method to evaluate the sterilization effect. As shown in Figs. 5a and b, when 200 μL of 1×10^9 CFU/mL Escherichia coli (*E. coli*) suspension was added to the TSA culture medium, both the H_2O_2 filter paper disc and the SAP filter paper disc formed clear and visible inhibition zones on the culture medium after 48 h. The areas of the inhibition zones for both were approximately the same. To verify the long-term sterilization effect of SAP, the filter paper discs were taken out of the culture medium at 72 h and then swabbed with 100 μL of Luria-Bertani broth. After 144 h of observation, it was found that the inhibition boundary line of the TSA culture medium with the H_2O_2 filter paper disc became blurry, and there were obvious colonies within the previous inhibition zone (indicated by the yellow circle in the image), SEM image of *E. coli* bacterial colonies was shown in Fig. S18 (Supporting information). However, in the case of the SAP filter paper disc, the boundary line remained clear, and no bacterial colony was observed within the inhibition zone. This shows that SAP has the advantage of long-term antibacterial.

To further confirm the long-term antibacterial effect of SAP with swelling H_2O_2, pre-treated filter paper discs were left in the environment for 6 h and then placed on TSA agar supplemented with 500 μL of 1×10^9 CFU/mL bacterial suspension. The growth of bacterial colonies in the agar was observed over time. After 48 h, the TSA agar treated with SAP filter paper discs exhibited clear inhibitory zones, while the TSA agar treated with H_2O_2 filter paper discs did not show significant inhibition. Continuous observation revealed that, even after 96 h of cultivation, the TSA agar treated

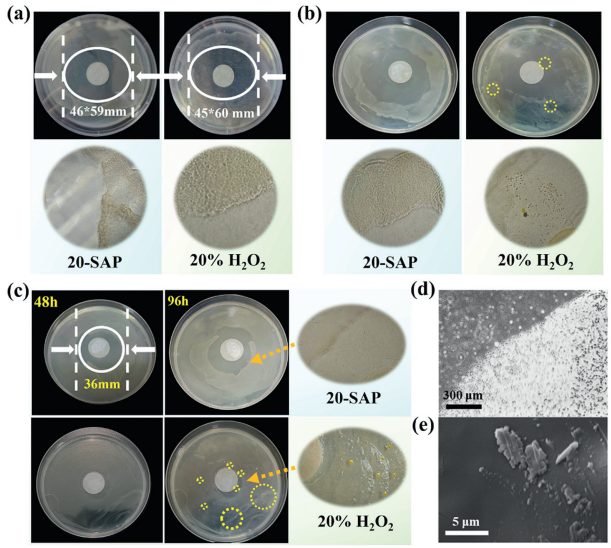

Fig. 5. (a) The bactericidal effect of 20-SAP and 20% H_2O_2 filter paper tablets for 48 h at 20 °C constant temperature. (b) After 72 h of sterilization, 100 μL of Luria-Bertani broth was added to TSA medium for 144 h of sterilization effect. (c) The treated filter paper tablets were placed on 1×10^9 CFU/mL TSA medium with 500 μL added, and sterilized at a constant temperature of 20 °C. (d) Image of sterilizing demarcation line microscope. (e) SEM image of *E. coli* after treatment.

with SAP filter paper discs still displayed distinct inhibitory zones. In contrast, the TSA agar treated with H_2O_2 filter paper discs exhibited abundant bacterial colonies, as illustrated in Fig. 5c. Photographs of the antibacterial zone boundaries treated with 20-SAP in Fig. 5c were captured using the Olympus IX73 microscope, as shown in Fig. 5d, revealing a clear boundary line of light and dark. The densely packed *E. coli* is observed on the dark side, while the bright side represents the interior of the antibacterial zone, where *E. coli* is no longer observable. The characterization of bacterial states in TSA culture medium through SEM reveals that, under the influence of H_2O_2, bacterial cells exhibit fragmentation, as illustrated in Fig. 5e.

To validate the broad applicability of storing H_2O_2 in hydrogels, in the follow-up experiment of this subject, the hydrogel prepared by acrylonitrile and acrylic ester (a kind of children's toy, bubble beads) was used for hydrogen peroxide storage. As shown in Fig. S19 (Supporting information), bubble beads also absorb the expanding hydrogen peroxide solution. At the same time, the SR of this commercial hydrogel decreases, and the AF increases with the increase of the absorbed hydrogen peroxide mass fraction. When this swollen commercial hydrogel is placed in ultra-pure water, the swollen hydrogel can still be released in the water.

In summary, hydrogels have been successfully employed for the storage of H_2O_2, demonstrating the capability to sustained release H_2O_2 through osmotic pressure without the need for additional stabilizers. H_2O_2 can maintain long-term stability within the hydrogel. After three days of agitation, SAP continued to effectively apply the sustained release of H_2O_2 in Fenton reactions, exhibiting equivalent performance to statically stored SAP. The hydrogel has been able to maintain its morphology under continuous vigorous oscillation conditions over a period of 3 days and can be stabilized under static conditions for >7 days, which meets the requirements for long-term transportation and storage. The mechanism of SAP storage and sustained release of H_2O_2 is mainly related to the osmotic pressure of the surrounding solution, ensuring the free and recyclable storage and release of H_2O_2 in the hydrogel. Furthermore, the sustained release effect of H_2O_2 in SAP has been demonstrated to exhibit advantages in Fenton reactions and long-term bacterial inactivation. The effective storage of H_2O_2 in hydrogels addresses the transportation challenges associated with H_2O_2 and the sustained release effect of H_2O_2 from hydrogels is expected to significantly enhance its utilization efficiency and promote its application in complex environments. Therefore, the storage of H_2O_2 in hydrogels has the potential to impact various fields, including agriculture, healthcare, biology, environment protect and so on.

Declaration of competing interest

The authors declare no competing financial interest.

CRediT authorship contribution statement

Zhuan Chen: Writing – original draft, Investigation, Data curation. **Bo Yang:** Writing – original draft, Investigation, Data curation. **Jun Li:** Resources. **Kun Du:** Resources. **Jiangchen Fu:** Resources. **Xiao Wu:** Resources. **Jiazhen Cao:** Resources. **Mingyang Xing:** Writing – review & editing, Supervision, Project administration, Funding acquisition, Formal analysis, Conceptualization.

Acknowledgments

This work was supported by National Natural Science Foundation of China (Nos. 22325602, 22176060) and Program of Shanghai Academic/Technology Research Leader (No. 23XD1421000). Project supported by Shanghai Municipal Science and Technology Major Project (No. 2018SHZDZX03) and the Program of Introducing Talents of Discipline to Universities (No. B16017). Science and Technology Commission of Shanghai Municipality (No. 20DZ2250400). Authors thank Research Center of Analysis and Test of East China University of Science and Technology for the help on the characterization.

Supplementary materials

Supplementary material associated with this article can be found, in the online version, at doi:10.1016/j.cclet.2024.110320.

References

[1] K. Zhang, M. Dan, J. Yang, et al., Adv. Funct. Mater. 33 (2023) 2302964.
[2] B. Puértolas, A. Hill, T. García, et al., Catal. Today 248 (2015) 115–127.
[3] J.H. Ji, Z.J. Wang, Q. Xu, et al., Chem. Eur. J. 29 (2023) e202203921.
[4] K. Zhang, L. Tian, J. Yang, et al., Angew. Chem. Int. Ed. 136 (2024) e202317816.
[5] S.L. Li, J.X. Ma, F. Xu, et al., Chem. Eng. J. 452 (2023) 139371.
[6] A. Wang, A. Bonakdarpour, D.P. Wilkinson, et al., Electrochim. Acta 66 (2012) 222–229.
[7] J.K. Edwards, B. Solsona, E.N. N, et al., Science 323 (2009) 1037–1041.
[8] M. Dan, R. Zhong, S. Hu, et al., Chem Catal. 2 (2022) 1919–1960.
[9] L. Tian, Z.J. Tang, L.Y. Hao, et al., Angew. Chem. 136 (2024) e202401434.
[10] Y. Ni, C.X. Zhou, M.Y. Xing, et al., Green Energy Environ. 9 (2023) 417–434.
[11] M. Kumasaki, J. Loss Prev. Process. Ind. 19 (2006) 307–311.
[12] J.M. Campos-Martin, G. Blanco-Brieva, J.L. Fierro, Angew. Chem. Int. Ed. 45 (2006) 6962–6984.
[13] F. Raza, H. Zafar, Y. Zhu, et al., Pharmaceutics 10 (2018) 16.
[14] I. Carayon, A. Gaubert, Y. Mousli, et al., Biomater. Sci. 8 (2020) 5589–5600.
[15] G. Sennakesavan, M. Mostakhdemin, L. Dkhar, et al., Polym. Degrad. Stab. 180 (2020) 109308.
[16] P. Kaur, R. Agrawal, F.M. Pfeffer, et al., J. Polym. Environ. 31 (2023) 1–18.
[17] R.H. Mu, B. Liu, X. Chen, et al., Environ. Technol. Innovation 20 (2020) 101107.
[18] W. Tanan, J. Panichpakdee, P. Suwanakood, et al., J. Ind. Eng. Chem. 101 (2021) 237–252.
[19] L. Guo, Y. Wang, M. Wang, et al., J. Cleaner Prod. 324 (2021) 129274.
[20] S. Das, G. Dalei, Sci. Total Environ. 875 (2023) 162660.
[21] S. Fertahi, I. Bertrand, M. Ilsouk, et al., Int. J. Biol. Macromol. 143 (2020) 153–162.
[22] F. Khan, M. Atif, M. Haseen, et al., J. Mater. Chem. B 10 (2022) 170–203.
[23] J.B. Yao, L.X. Shen, Z.R. Chen, et al., ACS Biomater. Sci. Eng. 8 (2022) 2066–2075.
[24] Z.J. Fei, N. Gupta, M.J. Li, et al., Sci. Adv. 9 (2023) eadg9933.
[25] E. Griswold, J. Cappello, H. Ghandehari, Adv. Drug Delivery. Rev. 191 (2022) 114579.
[26] J.J. Hu, Y.H. Chen, Y.Q. Li, et al., Biomaterials 112 (2017) 133–140.
[27] S. Sarkar, C. Hazra, M. Chatti, et al., RSC Adv. 2 (2012) 8269–8272.

[28] M.R. Vakili, W. Mohammed-Saeid, A. Aljasser, et al., Carbohydr. Polym. 255 (2021) 117332.
[29] M. Pourmadadi, S. Darvishan, M. Abdouss, et al., Ind. Crops Prod. 197 (2023) 116654.
[30] W.M. Cheng, X.M. Hu, Y.Y. Zhao, et al., e-Polymers 17 (2017) 95–106.
[31] Q. Zhang, K. Xu, P. Wang, Fibers Polym. 9 (2008) 271–275.
[32] Z. Zhang, P.R. Chen, X.F. Du, et al., Carbohydr. Polym. 102 (2014) 453–459.
[33] Y. Bao, J.Z. Ma, N. Li, Carbohydr. Polym. 84 (2011) 76–82.
[34] A. Ulu, S. Koytepe, B. Ates, Carbohydr. Polym. 153 (2016) 559–572.
[35] Y.S. Solanki, M. Agarwal, A. Gupta, et al., Sci. Total Environ. 807 (2022) 150601.
[36] P.J. Flory, Principles of Polymer Chemistry, Cornell University Press, 1953.
[37] R. Gouda, H. Baishya, Z. Qing, J. Dev. Drugs 6 (2017) 1–8.
[38] J. Cobby, M. Mayersohn, G.C. Walker, J. Pharm. Sci. 63 (1974) 732–737.
[39] Z. Chen, F.L. An, Y.Y. Zhang, et al., Proc. Natl. Acad. Sci. U. S. A. 120 (2023) e2305933120.
[40] Z. Chen, C. Lian, K. Huang, et al., Chin. Chem. Lett. 33 (2022) 1365–1372.